ChemComm

COMMUNICATION

View Article Online
View Journal | View Issue

Cite this: *Chem. Commun.*, 2025, **61**, 3143

Received 13th December 2024,
Accepted 21st January 2025

DOI: 10.1039/d4cc06539e

rsc.li/chemcomm

Potassium–telluroether interactions: structural characterisation and computational analysis†

Novan A. G. Gray, [a] James F. Britten[b] and David J. H. Emslie *[a]

Dissolution of the potassium complex [K(ATe$_2^{Tripp2}$)(dme)$_2$] (1-Te) in THF, layering with hexanes, and cooling to −30 °C afforded X-ray quality crystals of [K(ATe$_2^{Tripp2}$)(THF)$_3$] (2-Te). The K–TeR$_2$ distances in 2-Te are substantially shorter than those in 1-Te, and DFT and QTAIM calculations support the presence of K–TeR$_2$ interactions, providing the first unambiguous examples of s-block–telluroether bonding. Attempts to prepare bulk quantities of 2-Te afforded [K(ATe$_2^{Tripp2}$)(THF)$_2$] (3-Te), and further drying yielded [K(ATe$_2^{Tripp2}$)(THF)] (4-Te) and [K(ATe$_2^{Tripp2}$)]$_x$ (5-Te). The selenium analogues of 2-Te, 3-Te and 4-Te (2-Se, 3-Se and 4-Se), were also prepared, and 2-Te, 2-Se, 3-Se and 5-Te were crystallographically characterised.

In the chemistry of hard electropositive metal ions, soft donor ligands have proven valuable for the synthesis of luminescent zero-field single-molecule magnets (SMMs),[1] as a means to promote FLP reactivity,[2] for preferential complexation of actinide *versus* lanthanide elements with potential applications in nuclear fuel reprocessing,[3–11] as ligands in metal-containing CVD precursors,[12,13] and to access high nuclearity clusters.[14] Soft donor ligands can also offer benefits in electropositive metal catalysis. For example, neodymium complexes with a pendent phosphine sulfide were substantially more active isoprene polymerization catalysts than phosphine oxide analogues,[15] and group 4 complexes of ligands incorporating phosphine or thioether donors exhibited far higher ethylene polymerization activity than analogues incorporating ether or quinoline donors.[16] Also, in a more general sense, integration of both hard and soft donors into multidentate ligand frameworks has been shown to be a powerful strategy to access electropositive metal complexes with unique properties and reactivity stemming from an atypical electronic environment,[16–24] and an enhanced understanding of the scope and nature of hard metal–soft donor interactions can further these applications.

Interactions between s-block metals and telluroether ligands push the boundaries of hard–soft mismatch, but unambiguous examples of such interactions have thus far proven elusive. For example, the [18]aneO$_4$Te$_2$ (1,4,10,13-tetraoxa-7,16-ditellura-cyclooctadecane) macrocycle failed to react with MI$_2$ (M = Ca or Sr), whereas analogous reactions with [18]aneO$_4$Se$_2$ afforded [MI$_2$([18]aneO$_4$Se$_2$)] (M = Ca and Sr).[25] Additionally, while the selenoether-ligated alkaline earth dications [M([18]aneO$_4$Se$_2$)(MeCN)$_2$][BAr$^F_4$]$_2$ (M = Mg, Ca, Sr), [Ba([18]aneO$_4$Se$_2$)(acacH)(MeCN)][BAr$^F_4$]$_2$, [Sr(H$_2$O)$_3$([18]ane-O$_4$Se$_2$)]I$_2$ and [Mg(κ^3-[18]aneO$_4$Se$_2$)(H$_2$O)$_2$(MeCN)][BAr$^F_4$]$_2$[26] and the group 1 selenoether complexes [M([18]ane-O$_4$Se$_2$)][B{C$_6$H$_3$(CF$_3$)$_2$-3,5}$_4$] (M = Na and K)[27] have been reported, telluroether analogues are unknown. More broadly, telluroether complexes of electropositive lanthanide or actinide elements are also unknown.

Recently, we reported the lithium and potassium complexes [{Li(ASe$_2^{Ph2}$)}$_2$] and [K(ASe$_2^{Ar2}$)(dme)$_2$] {ASe$_2^{Ar2}$; 4,5-bis(arylselenido)-2,7,9,9-tetramethylacridanide; Ar = phenyl or 2,4,6-triisopropylphenyl (**1-Se**)}, which feature unique or uncommon s-block metal–selenoether interactions.[28,29] The ASe$_2^{Ar2}$ ligand in these compounds is a monoanionic SeNSe-donor pincer ligand which encourages κ^3-coordination by direct attachment of the selenium donors to a rigid acridanide ligand backbone. We also reported the telluroether analogue, [K(ATe$_2^{Tripp2}$)(dme)$_2$] (**1-Te**).[28] However, the K–TeR$_2$ distances in the solid-state structure of this compound are approximately 0.39 Å longer than those in the selenoether analogue, even though the covalent radius of tellurium is only 0.18 Å larger than that of selenium.[30] Furthermore, DFT and QTAIM calculations on a model of [K(ATe$_2^{Tripp2}$)(dme)$_2$] in which the K–Te distances are constrained to crystallographic values did not yield K–Te bond critical points (BCPs), and other computational metrics suggested minimal interaction between K and Te. Therefore, although a shallow potential energy surface may allow K–Te interactions to form in solution, the solid-state structure of [K(ATe$_2^{Tripp2}$)(dme)$_2$] cannot be considered to

[a] *Department of Chemistry and Chemical Biology, McMaster University, Hamilton, Ontario, L8S 4M1, Canada. E-mail: emslied@mcmaster.ca*
[b] *McMaster Analytical X-ray Diffraction Facility, McMaster University, Hamilton, Ontario, L8S 4M1, Canada*

† Electronic supplementary information (ESI) available. CCDC 2408834–2408837. For ESI and crystallographic data in CIF or other electronic format see DOI: https://doi.org/10.1039/d4cc06539e

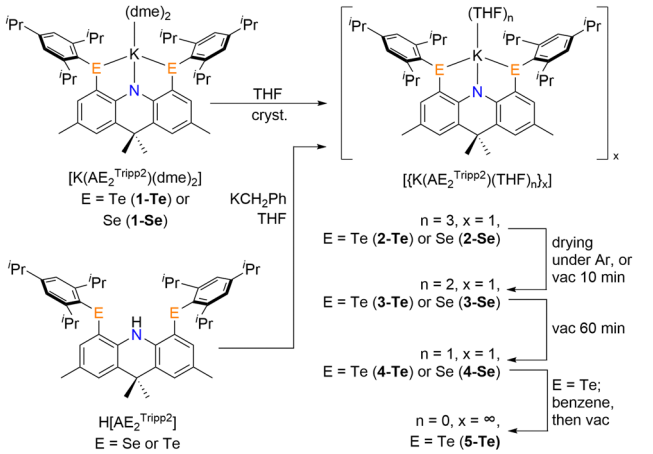

Scheme 1 Syntheses of potassium telluroether and selenoether complexes.

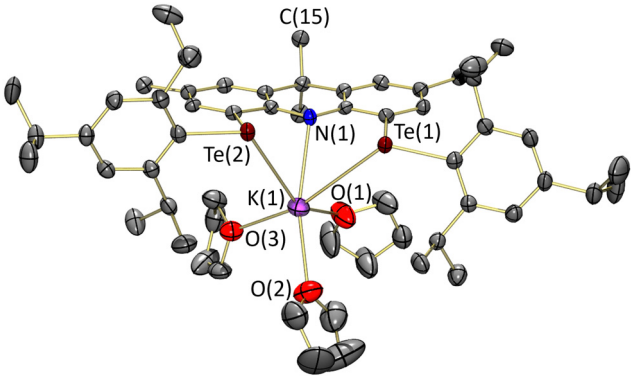

Fig. 1 X-ray crystal structure of [K(ATe$_2^{Tripp2}$)(THF)$_3$] (**2-Te**). One part of a 50 : 50 two-part THF backbone disorder (associated with the THF containing O(2)) is shown. Hydrogen atoms are omitted for clarity. Ellipsoids are drawn at 50% probability.

feature significant K–TeR$_2$ interactions, and unambiguous examples of s-block–telluroether compounds remain elusive.

Herein, we report the synthesis and solid-state structure of the THF-coordinated analogue of **1-Te**, [K(ATe$_2^{Tripp2}$)(THF)$_3$] (**2-Te**), featuring K–Te distances that are substantially shorter (by ∼0.3 Å) than those in the dme analogue, and quantum chemical calculations which confirm K–Te bonding in **2-Te**. Analogues of **2-Te** in which potassium is coordinated to 2, 1 or 0 equivalents of THF, and selenoether analogues of these complexes (where potassium is coordinated to 3, 2 or 1 equivalents of THF) are also reported.

Dissolution of dme-coordinated [K(ATe$_2^{Tripp2}$)(dme)$_2$] (**1-Te**) in THF, layering with hexanes and cooling to −30 °C overnight furnished yellow block-shaped X-ray quality crystals of [K(ATe$_2^{Tripp2}$)(THF)$_3$] (**2-Te**); Scheme 1. In the solid-state, potassium is κ^3*TeNTe*-coordinated to the ATe$_2^{Tripp2}$ ligand as well as three molecules of THF, affording a distorted octahedral geometry (Fig. 1).[31,32] The K–O distances range from 2.584(5) to 2.693(5) Å, and the K–N distance of 2.824(4) Å is comparable to that found in the X-ray structure of [K(ATe$_2^{Tripp2}$)(dme)$_2$] (2.842(3) Å).[28] Most interestingly, the K–Te distances in **2-Te** are 3.496(2) and 3.639(2) Å, which are 0.312 and 0.277 Å shorter than those in the dme analogue (see Table 1). The substantial difference in the K–Te distances in **1-Te** and **2-Te** is likely due to a shallow potential energy surface that is readily influenced by crystal packing forces.

Drying samples of **2-Te** under argon, or under vacuum for 10 minutes resulted in loss of one equivalent of THF to afford [K(ATe$_2^{Tripp2}$)(THF)$_2$] (**3-Te**; Scheme 1), as determined by ^{1}H NMR integration and combustion elemental analysis. Compound **3-Te** was also isolated by deprotonation of H[ATe$_2^{Tripp2}$] using KCH$_2$Ph in THF, followed by evaporation to dryness *in vacuo*. Further loss of THF from **3-Te** was observed after longer exposure (an additional 60 minutes) of solid samples to vacuum, affording [K(ATe$_2^{Tripp2}$)(THF)] (**4-Te**; Scheme 1). Moreover, repetitive dissolution of **4-Te** in benzene and removal of volatiles *in vacuo* afforded THF-free [K(ATe$_2^{Tripp2}$)]$_x$ (**5-Te**; Scheme 1). An X-ray quality crystal of **5-Te** was obtained by layering an *o*-difluorobenzene solution of **4-Te** with pentane and cooling to −30 °C for 1 month. In the solid state, **5-Te** (Fig. 2) is a 1-dimensional coordination polymer in which potassium bridges between ATe$_2^{Tripp2}$ ligands. The K–N distances are 2.76(1) and 2.81(1) Å, and there are three short (3.517(4)–3.680(4) Å) K–Te distances which are only slightly longer than those in **2-Te** (*vide supra*). There is also one longer K–Te distance (K(1)–Te(2) = 4.265(4) Å) that is outside of the range for a K–Te interaction. Interestingly, despite the polymeric structure of **5-Te** in the solid state, it is soluble in benzene, indicating that the 1D-chains can easily be disrupted (presumably to form monomers in which potassium is stabilized through interactions with benzene and/or flanking hydrocarbon groups).

Attempts were also made to prepare a selenoether analogue of **2-Te** by dissolving [K(ASe$_2^{Tripp2}$)(dme)$_2$] (**1-Se**) in THF, layering with hexanes, and cooling to −30 °C. This afforded yellow plate-like crystals, several of which were analyzed. One of these crystals could successfully be modelled as [K(ASe$_2^{Tripp2}$)(THF)$_3$]·hexane (**2-Se**·hexane; Fig. S1, ESI†), whereas another could be modelled as [K(ASe$_2^{Tripp2}$)(THF)$_2$] (**3-Se**; Fig. 3). However, both crystals, which share the same $P2_1/c$ space group with very similar unit cell *a* and *b* axis dimensions,‡ show significant diffuse scattering along the *c* axis, suggestive of incommensurate structures[33] resulting from intergrowth of **2-Se**·hexane with **3-Se**.§ As a result, the *R*-factors are high (17–20%) and C–C bond precision is relatively low (>0.02 Å). Nevertheless, the standard deviations for the K–Se, K–O and K–N distances are sufficiently low to permit meaningful discussion.

Potassium is distorted octahedral in **2-Se**, and distorted square pyramidal (vacant octahedral) in **3-Se**.[32] The K–N distances in **2-Se** and **3-Se** are unremarkable at 2.82(1) and 2.72(2) Å, respectively, and the K–O distances are 2.67(1)–2.79(1) Å in **2-Se** and 2.70(2) and 2.73(2) Å in **3-Se**. The K–Se distances in **2-Se** and **3-Se** are similar, at 3.397(4) and 3.472(4) Å in the former, and 3.347(5) and 3.466(5) Å in the latter, and the average K–Se distances of 3.435(4) and 3.407(5) Å in these compounds, respectively, are only slightly shorter than that for dme-coordinated **1-Se** (3.469(2) Å; see Table 1).[28] It is also

Table 1 Tabulated K–E (E = Te or Se), K–N and K–O bond distances in the X-ray crystal structures of **1-Te**, **2-Te**, **5-Te**, **1-Se**, **2-Se**, and **3-Se**

Complex	K–E distances (E = Te or Se) (Å)	K–N distances (Å)	K–O distances (Å)
1-Te[28]	3.808(1), 3.916(1)	2.842(3)	2.660(3)–2.865(3)
2-Te	3.496(2), 3.639(2)	2.824(4)	2.584(5)–2.693(5)
5-Te	3.517(4), 3.677(4), 3.680(4)	2.76(1), 2.81(1)	n.a.
1-Se[28]	3.339(2), 3.419(2), 3.484(2), 3.633(2)[a]	2.801(4), 2.840(3)[a]	2.701(3)–3.13(1)[a]
2-Se	3.397(4), 3.472(4)	2.82(1)	2.67(1)–2.79(1)
3-Se	3.347(5), 3.466(5)	2.72(2)	2.70(2), 2.73(2)

[a] Two independent molecules are present in the asymmetric unit.

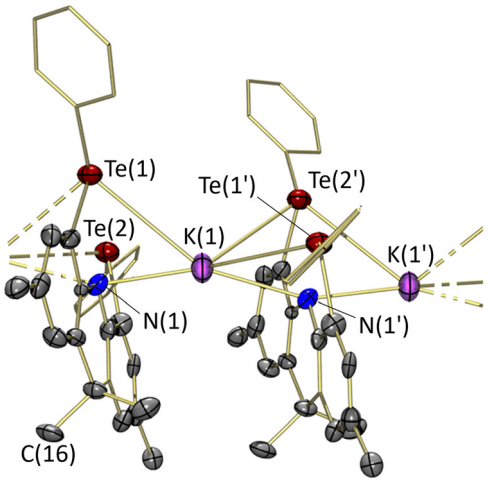

Fig. 2 X-ray crystal structure of $[K(ATe_2^{Tripp2})]_x$ (**5-Te**). A two-monomer segment of the 1D polymeric structure is shown. Aryl substituents are shown in wireframe and hydrogen atoms and isopropyl groups are omitted for clarity. Ellipsoids are drawn at 50% probability.

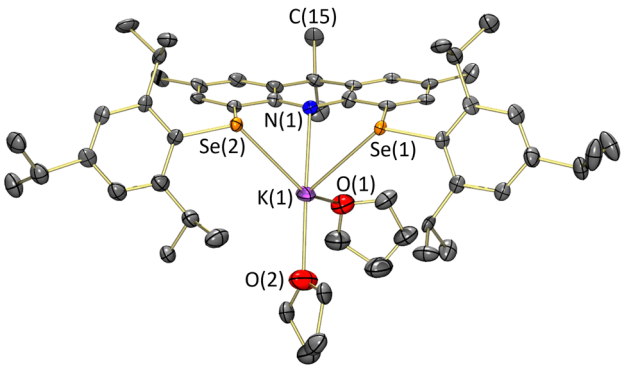

Fig. 3 X-ray crystal structure of $[K(ASe_2^{Tripp2})(THF)_2]$ (**3-Se**; with diffuse scattering along the *c*-axis suggesting intergrowth of **3-Se** (major) with **2-Se**·hexane (minor). Hydrogen atoms are omitted for clarity. Ellipsoids are drawn at 50% probability.

notable that the average K–Se distance in **2-Se** (3.435(4) Å) is 0.133 Å shorter than the average K–Te distance in **2-Te** (3.568(2) Å), which is less than the difference in the covalent radii of selenium and tellurium (0.18 Å).[30]

Pure **3-Se** was obtained by drying samples of **2-Se**/**3-Se** under argon or *in vacuo* for 10 minutes. However, as observed for the telluroether analogue, additional exposure of **3-Se** to vacuum resulted in further loss of THF, affording $[K(ASe_2^{Tripp2})(THF)]$ (**4-Se**; Scheme 1).¶

The ^{1}H and $^{13}C\{^1H\}$ NMR spectra of **3-Te**–**5-Te**, **3-Se** and **4-Se** in C_6D_6 display ligand-based resonances indicative of ligand top-bottom and side-to-side symmetry on the NMR timescale, with chemical shifts that are nearly identical ($\Delta\delta$ ^{1}H $<$ 0.06 ppm, $\Delta\delta$ ^{13}C $<$ 0.03 ppm) to those of the bis-dme analogues (**1-Te** or **1-Se**). Similarly, the ^{125}Te NMR chemical shifts of **3-Te**, **4-Te** and **5-Te**, and the ^{77}Se NMR chemical shifts of **3-Se** and **4-Se**, are within ~1 ppm of the dme analogues.[28] It is also notable that the ^{1}H and ^{13}C NMR signals for THF in compounds **3**–**4** in C_6D_6 are only very slightly shifted relative to free THF ($\Delta\delta$ ^{1}H $<$ 0.03 ppm, $\Delta\delta$ ^{13}C $<$ 0.09 ppm), suggestive of substantial (or complete) THF dissociation in solution. This contrasts the situation for **1-Te** and **1-Se**, wherein notable shifts in the dme ^{1}H NMR ($\Delta\delta$ 0.13–0.19 ppm) and ^{13}C NMR ($\Delta\delta$ 0.02–0.41 ppm) resonances were observed in C_6D_6.[28]

Quantum chemical calculations (ADF, gas-phase, all-electron, PBE, D3-BJ, TZ2P, ZORA) were carried out to confirm the presence of K–E interactions in **2-Te** and **2-Se**. These calculations were performed on models of **2-Te** and **2-Se** in which the 2,4,6-triisopropylphenyl groups have been replaced by 2,6-diisopropylphenyl groups: $[K(ATe_2^{Dipp2})(THF)_3]$ (**2-Te***) and $[K(ASe_2^{Dipp2})(THF)_3]$ (**2-Se***). Relative to the solid-state structures, one of the K–Te distances in **2-Te*** is overestimated by 0.09 Å while the other is within 0.001 Å of the crystallographic value, and the K–Se distances in **2-Se*** are within 0.04 Å of those in **2-Se**. The K–E (E = Te or Se) Mayer bond orders in **2-Te*** and **2-Se*** are 0.08–0.10 and 0.07–0.08, respectively, supporting the presence of K–ER_2 bonding in both complexes, with minimal covalent contributions. Furthermore, Quantum Theory of Atoms in Molecules (QTAIM) bond critical points (BCPs) were located between potassium and both chalcogen donors in **2-Te*** and **2-Se***. Small positive values of the total energy density of Cramer and Kraka at the BCP (H_b; 0.0010 au in **2-Te***; 0.0013 au in **2-Se***) and low bond delocalization index (δ) values (0.0678–0.0736 in **2-Te***; 0.0671–0.0673 in **2-Se***) are consistent with primarily electrostatic bonding. Additionally, NBO analysis revealed metal orbital contributions of less than 1.0% in the chalcogen-based NLMO (natural localized molecular orbital) lone pairs in **2-Te*** and **2-Se***, consistent with predominantly electrostatic bonding.

In summary, the s-block–chalcogenoether complexes $[K(ATe_2^{Tripp2})(THF)_x]$ (x = 0–3) and $[K(ASe_2^{Tripp2})(THF)_x]$ (x = 1–3) have been synthesized, and DFT and QTAIM calculations on

$[K(AE_2{}^{Dipp2})(THF)_3]$ (E = Te or Se) confirmed the presence of K–ER_2 bonding, with primarily ionic character. $[K(ATe_2{}^{Tripp2})(THF)_3]$ is the first unambiguous example of an s-block telluroether complex, and the K–TeR_2 interactions in this work will provide a valuable point of comparison for other electropositive metal–TeR_2 interactions, such as those involving early transition metals or f-elements.

D. J. H. E. thanks NSERC of Canada for a Discovery Grant, and N. A. G. G. thanks the Government of Ontario for an Ontario Graduate Scholarship (OGS). We are also grateful to Dr Jeffrey S. Price for assistance with X-ray crystallography, and Dr Ignacio Vargas-Baca for helpful discussions on quantum chemical calculations.

Data availability

Data supporting this article is included in the ESI.† Crystallographic data for **2-Te**, **2-Se**, **3-Se** and **5-Te** has been deposited at the CCDC with deposition numbers 2408834–2408837, respectively.

Conflicts of interest

There are no conflicts to declare.

Notes and references

‡ The *a*, *b* and *c* unit cell dimensions are 9.312(5), 18.550(9) and 35.565(16) Å, respectively, in the structure consisting primarily of **2-Se**·hexane, and 9.342(4), 18.461(7) and 29.140(8) Å in the structure consisting primarily of **3-Se**.
§ Attempts to prepare X-ray quality single crystals of pure **3-Se** by dissolving **3-Se** in toluene or *o*-difluorobenzene, layering with hexanes and cooling to −30 °C were unsuccessful.
¶ Attempts to prepare (a) pure $[K(ASe_2{}^{Tripp2})(THF)_2]$ (**3-Se**) by dissolving $[K(ASe_2{}^{Tripp2})(dme)_2]$ (**1-Se**) in THF followed by evaporation of the volatiles (×3), or (b) $[K(ASe_2{}^{Tripp2})]_x$ by dissolving $[K(ASe_2{}^{Tripp2})(THF)]$ (**4-Se**) in benzene followed by evaporation of the volatiles (×2) consistently led to mixtures of the target products (**3-Se** or $[K(ASe_2{}^{Tripp2})]_x$) and pro-ligand in an approximate 1 : 0.4 ratio (Fig. S17 and S18, ESI†). Therefore, these reactions were not pursued further.

1 R. Marin, D. A. Gálico, R. Gayfullina, J. O. Moilanen, L. D. Carlos, D. Jaque and M. Murugesu, *J. Mater. Chem. C*, 2022, **10**, 13946.
2 J. Langer, I. Kosygin, R. Puchta, J. Pahl and S. Harder, *Chem. – Eur. J.*, 2016, **22**, 17425.
3 N. P. Bessen, J. A. Jackson, M. P. Jensen and J. C. Shafer, *Coord. Chem. Rev.*, 2020, **421**, 213446.
4 P. R. Zalupski, J. R. Klaehn and D. R. Peterman, *Solvent Extr. Ion Exch.*, 2015, **33**, 523.
5 I. Lehman-Andino, J. Su, K. E. Papathanasiou, T. M. Eaton, J. W. Jian, D. Dan, T. E. Albrecht-Schmitt, C. J. Dares, E. R. Batista, P. Yang, J. K. Gibson and K. Kavallieratos, *Chem. Commun.*, 2019, **55**, 2441.
6 L. Karmazin, M. Mazzanti and J. Pecaut, *Chem. Commun.*, 2002, 654.
7 A. J. Gaunt and M. P. Neu, *C. R. Chim.*, 2010, **13**, 821.
8 A. J. Gaunt, B. L. Scott and M. P. Neu, *Angew. Chem., Int. Ed.*, 2006, **45**, 1638.
9 C. A. P. Goodwin, A. W. Schlimgen, T. E. Albrecht-Schönzart, E. R. Batista, A. J. Gaunt, M. T. Janicke, S. A. Kozimor, B. L. Scott, L. M. Stevens, F. D. White and P. Yang, *Angew. Chem., Int. Ed.*, 2021, **60**, 9459.
10 N. P. Bessen, I. A. Popov, C. R. Heathman, T. S. Grimes, P. R. Zalupski, L. M. Moreau, K. F. Smith, C. H. Booth, R. J. Abergel, E. R. Batista, P. Yang and J. C. Shafer, *Inorg. Chem.*, 2021, **60**, 6125.
11 C. A. P. Goodwin, R. W. Adams, A. J. Gaunt, S. K. Hanson, M. T. Janicke, N. Kaltsoyannis, S. T. Liddle, I. May, J. L. Miller, B. L. Scott, J. A. Seed and G. F. S. Whitehead, *J. Am. Chem. Soc.*, 2024, **146**, 10367.
12 A. L. Hector, M. Jura, W. Levason, S. D. Reid and G. Reid, *New J. Chem.*, 2009, **33**, 641.
13 V. Sethi, D. Runacres, V. Greenacre, L. Shao, A. L. Hector, W. Levason, C. H. de Groot, G. Reid and R. Huang, *J. Mater. Chem. A*, 2023, **11**, 9635.
14 J. Langer, B. Maitland, S. Grams, A. Ciucka, J. Pahl, H. Elsen and S. Harder, *Angew. Chem., Int. Ed.*, 2017, **56**, 5021.
15 O. A. Basalova, A. O. Tolpygin, T. A. Kovylina, A. V. Cherkasov, G. K. Fukin, K. A. Lyssenko and A. A. Trifonov, *Organometallics*, 2021, **40**, 2567.
16 D. C. H. Oakes, B. S. Kimberley, V. C. Gibson, D. J. Jones, A. J. P. White and D. J. Williams, *Chem. Commun.*, 2004, 2174.
17 R. J. Long, V. C. Gibson, A. J. P. White and D. J. Williams, *Inorg. Chem.*, 2006, **45**, 511.
18 R. J. Burford, A. Yeo and M. D. Fryzuk, *Coord. Chem. Rev.*, 2017, **334**, 84.
19 T. Cantat, C. R. Graves, B. L. Scott and J. L. Kiplinger, *Angew. Chem., Int. Ed.*, 2009, **48**, 3681.
20 L. C. Liang, *Coord. Chem. Rev.*, 2006, **250**, 1152.
21 L. S. Merz, J. Ballmann and L. H. Gade, *Eur. J. Inorg. Chem.*, 2020, 2023.
22 D. P. Solowey, M. V. Mane, T. Kurogi, P. J. Carroll, B. C. Manor, M. H. Baik and D. J. Mindiola, *Nat. Chem.*, 2017, **9**, 1126.
23 S. Senthil, S. Kwon, D. Fehn, H. Im, M. R. Gau, P. J. Carroll, M. H. Baik, K. Meyer and D. J. Mindiola, *Angew. Chem., Int. Ed.*, 2022, **61**, e202212488.
24 A. V. Zabula, Y. S. Qiao, A. J. Kosanovich, T. Cheisson, B. C. Manor, P. J. Carroll, O. V. Ozerov and E. J. Schelter, *Chem. – Eur. J.*, 2017, **23**, 17923.
25 P. Farina, W. Levason and G. Reid, *Dalton Trans.*, 2013, **42**, 89.
26 W. Levason, D. Pugh, J. M. Purkis and G. Reid, *Dalton Trans.*, 2016, **45**, 7900.
27 M. J. D. Champion, W. Levason, D. Pugh and G. Reid, *Dalton Trans.*, 2015, **44**, 18748.
28 N. A. G. Gray, I. Vargas-Baca and D. J. H. Emslie, *Inorg. Chem.*, 2023, **62**, 16974.
29 N. A. G. Gray, J. S. Price and D. J. H. Emslie, *Chem. – Eur. J.*, 2022, **28**, e202103580.
30 B. Cordero, V. Gómez, A. E. Platero-Prats, M. Revés, J. Echeverría, E. Cremades, F. Barragán and S. Alvarez, *Dalton Trans.*, 2008, 2832.
31 S. Alvarez, D. Avnir, M. Llunell and M. Pinsky, *New J. Chem.*, 2002, **26**, 996.
32 S. Alvarez, P. Alemany, D. Casanova, J. Cirera, M. Llunell and D. Avnir, *Coord. Chem. Rev.*, 2005, **249**, 1693.
33 S. van Smaalen, *Crystallogr. Rev.*, 1995, **4**, 79.

